PHYSICAL REVIEW B VOLUME 2, NUMBER 6 15 SEPTEMBER 1970

ESR of Pb^{3+} Centers in ThO_2 †

J. L. Kolopus
Solid State Division, Oak Ridge National Laboratory, Oak Ridge, Tennesee 37830

and

C. B. Finch
Metals and Ceramics Division, Oak Ridge National Laboratory, Oak Ridge, Tennessee 37830

and

M. M. Abraham
Solid State Division, Oak Ridge National Laboratory, Oak Ridge, Tennessee 37830
(Received 27 October 1969; revised manuscript received 22 January 1970)

Spectra of Pb^{3+} in sites having cubic and axial symmetry have been identified in ThO_2 crystals grown from a PbF_2-based solvent which have been irradiated with electrons or γ rays. That part of the spectra arising from the 20%-abundant ^{207}Pb isotope ($I=\frac{1}{2}$) is characterized by a large zero-field hyperfine splitting. The Pb^{3+} center with $\langle 111\rangle$ axial symmetry shows a superhyperfine interaction with a ^{19}F nucleus. Part of this spectrum has previously been attributed to the F center in ThO_2. After exposure to ionizing radiation, no centers were detected in ThO_2 crystals grown from a $Li_2O \cdot 2WO_3$-based flux. Neutron irradiation of all crystals produced another center with $\langle 100\rangle$ axial symmetry.

INTRODUCTION

Electron spin resonance (ESR) investigations of irradiated ThO_2, which has the cubic fluorite structure, have previously been made by several investigators.[1,2] In the present work, crystals which have been grown in PbF_2-, PbO-, and $Li_2O \cdot 2WO_3$-based solvents were irradiated with ^{60}Co γ rays, 2-MeV electrons, and neutrons. The number and types of centers which are observed are found to be dependent not only on the type of irradiation, but also on the flux in which the crystal was grown.

EXPERIMENTAL

Single crystals of ThO_2 were grown at this laboratory by solvent volatilization (in air) from (a) PbF_2-B_2O_3-ThO_2 and (b) PbO-B_2O_3-ThO_2 solutions at ~ 1620 K.[3] The crystals from (a) have a well-developed cubic {100} habit; those from (b) are flaky and appear rhombohedral in form. Crystals from both (a) and (b) exhibit a slight orange discoloration after growth. Spectrographic analysis of the crystals from (a) revealed the presence of 500 ppm by weight of Pb impurity. Crystals grown from a PbF_2-based solution were obtained from Norton Industries, and additional ThO_2 crystals were grown at this laboratory from $Li_2O \cdot 2WO_3$-B_2O_3-ThO_2 solution.[4] The latter crystals are clear and colorless and have a {111} cubic growth habit. Spectrographic analysis showed no detectable Pb impurity, but about 100 ppm by weight of tungsten was detected.

The ionizing radiations used for our experiments were performed at room temperature using ^{60}Co γ rays with a flux of 3×10^6 R/h or by 2-MeV electrons at either 300 or 77 K. Both types of irradiation produced the same spectra at the dose levels given in this experiment, and no differentiation between these two types of irradiations will be made in the following discussion. The neutron irradiations were carried out in tube 1-F-12 of the Oak Ridge Research Reactor (neutron flux > 1.0 MeV ~ 3×10^{13} N/cm^2/sec) with the sample in contact with cooling water at 320 K. Some data were obtained from a sample which had been irradiated at 130 K in the Bulk Shielding Reactor at the ORNL and which was observed at 77K without an intervening warmup to room temperature.

The ESR investigations were carried out at X band using two separate spectrometers. One, employing a Varian V-4531 rectangular cavity with 100 kHz modulation, was used at 77 K and higher temperatures, while the other, employing a TE_{011} cylindrical cavity with 2 kHz modulation, was used for temperatures below 77 K. The hyperfine constants for $^{207}Pb^{3+}$ were measured at 77 K. The spin Hamiltonian used to fit the data was

$$\mathcal{H} = \beta \vec{H} \cdot \overleftrightarrow{g} \cdot \vec{S} + \vec{I} \cdot \overleftrightarrow{A} \cdot \vec{S} + \vec{I}_F \cdot \overleftrightarrow{A}_F \cdot \vec{S} \quad ,$$

where for $^{207}Pb^{3+}$, $I=S=\frac{1}{2}$, and the last term describes the superhyperfine interaction with an adjacent fluorine nucleus with $I_F=\frac{1}{2}$.

RESULTS

Before irradiation, there were no observable ESR spectra in any of the differently grown ThO_2 crystals. After room-temperature irradiation with β rays or γ rays, the crystals grown from the Pb-based solvents showed a deeper coloration, while the $Li_2O \cdot 2WO_3$-grown crystals remained colorless. No ESR signals were observed in the latter crystals, whereas, several were detected in the former (Fig. 1).

The spectrum identified as due to Pb^{3+} in a cubic site was observed only in crystals grown from the Pb-based solvents and consisted of a single isotropic line with $g = 1.9666 \pm 0.0006$ and a high-field isotropic line which arises from the 20.82% abundant ^{207}Pb isotope with $I = \frac{1}{2}$ (heavy arrow, Fig. 2). Because the hyperfine interaction constant $A = 13\,400 \pm 50$ G (1.230 cm^{-1}) is so large, the position of the high-field hyperfine lines must be determined for a system in which the electron and nuclear spins couple together (see the Appendix). The intensity of the isotropic hyperfine line belonging to the cubic Pb^{3+} spectrum at 5470 G relative to that of the line near $g = 2$ (which arises from the even-even isotopes of Pb) agreed well with the isotopic abundances. At 4.2 and 1.5 K the high-field $^{207}Pb^{3+}$ line was reduced in intensity, indicating that the absolute sign of A is positive. Schoemaker and Kolopus[5] identified the spectrum of Pb^{3+} in KCl by using samples enriched with ^{207}Pb. Similar supporting evidence for the ThO_2 work was obtained from neutron irradiated samples in the following way.

^{208}Pb is a doubly magic nucleus and therefore the neutron capture cross section for ^{207}Pb to even much larger than those for the other Pb isotopes. After neutron irradiation, the intensity of the high-field ^{207}Pb hyperfine line decreased, while the intensity of the line near $g = 2$ increased accordingly as a result of the net conversion of ^{207}Pb to even isotopes. This experiment served the same purpose as enriching the sample and was more readily done with the samples already in hand.

Additional confirmation was obtained from data taken at room temperature at 34 GHz. The position of the isotropic high-field line at about 17.0 kG agrees with formula (A1) for the line designated H_1. The spectrum of Pb^{3+} was also seen in CeO_2 crystals which are isomorphous to ThO_2 and which were grown from a PbF_2-based solvent. The spectrum was considerably weaker than that observed in ThO_2 for a given sample size and gamma dose but was sufficiently strong to measure the g value as $g = 1.9649 \pm 0.0008$ with a hyperfine splitting constant $A = 13\,130 \pm 50$ G (1.20 cm^{-1}). Only the isotropic Pb^{3+} spectrum was observed in the CeO_2 samples. A second Pb^{3+} spectrum exhibiting $\langle 111 \rangle$ axial symmetry involving an interaction of the Pb^{3+} with a nucleus with spin $I = \frac{1}{2}$ was observed in crystals grown from the PbF_2-based solvent. The absence of this center in crystals grown from a PbO-based solvent indicated that this was an interaction with a ^{19}F nucleus in one of the eight nearest-neighbor oxygen sites. The g values were $g_\parallel = 1.9704 \pm 0.0007$ and $g_\perp = 1.9637 \pm 0.0007$, while the hyperfine splitting constants were $A_\parallel = 1.194 \pm 0.010$ cm^{-1} and $A_\perp = 1.181 \pm 0.010$ cm^{-1}. The superhyperfine splitting of the Pb^{3+} lines could be fitted to the expression $\Delta H = a + b\,[3\cos^2(\theta - 1)]$, where $a = 14.5$ G and $b = 3.0$ G, corresponding to $(A_F)_\parallel = a + 2b = 18.9 \pm 0.5 \times 10^{-4}$ cm^{-1}, and $(A_F)_\perp = a - b = 10.5 \pm 0.5 \times 10^{-4}$ cm^{-1}.

At room temperature, the isotropic Pb^{3+} spectrum had a linewidth of 8–9 G, while the axial lines were ~15 G wide. Lowering the temperature narrowed the lines considerably so that at 77 K the lines of both spectra were ~2.5 G wide, while at 20 and 4.2 K, the isotropic line had narrowed to ~0.5 G and the axial lines to ~2 G. As the microwave power was increased, the Pb^{3+}-F^- spectrum saturated before the isotropic Pb^{3+} spectrum. At 4.2 K, an unusually large cross relaxation between the superhyperfine lines of the $\langle 111 \rangle$ axial spectrum was observed.

All the ThO_2 crystals, regardless of the growth solution used, showed a new center after neutron irradiation at 320 K with various doses up to a total of 1.7×10^{19} neutrons/cm^2. This center possessed $\langle 100 \rangle$ axial symmetry with $g_\parallel = 1.812 \pm 0.001$ and $g_\perp = 1.925 \pm 0.001$. The linewidths at 4.2 K were 4–5 G; although the crystals used were definitely single, the lines which were single when the applied magnetic field was perpendicular to the axis of symmetry split into two lines separated by about 3 G with $\vec{H}$ parallel to this axis. We interpret this to indicate the presence of two defects with slightly different $g_\parallel$ values but, within experimental error, equal $g_\perp$ values. For a given neutron dose, this spectrum was stronger in the crystals grown from the $Li_2O \cdot 2WO_3$ solvent. One crystal which was neutron irradiated at 130 K to a total dose of 2×10^{16} neutrons/cm^2 and observed at 77 K without warming showed, in addition to the center just mentioned, still another center with $\langle 111 \rangle$ axial symmetry having $g_\parallel = 2.003$ and $g_\perp = 2.095$. After warming to room temperature, the latter center annealed out. A summary of the spin Hamiltonian parameters for the principal spectra observed after various irradiations is given in Table I. Other weaker lines were observed after β irradiation but were not measured because of their low intensity.

DISCUSSION

Before irradiation, none of the crystals used in this investigation showed any detectable ESR spec-

FIG. 1. ESR spectrum of electron irradiated ThO_2 showing the cubic $^{even}Pb^{3+}$ line (arrow) and the ⟨111⟩ axial $^{even}Pb^{3+}$ lines (labeled A and B) which are split by a ^{19}F interaction. The peak-to-peak intensities of these lines do not exactly follow the indicated degeneracies because of a variation of the linewidths with angle. The lines labeled A are those previously identified as the F-center spectrum in ThO_2.

tra. After β or γ irradiation, only those crystals which were grown in Pb-containing solvents showed any visible coloration or any ESR spectra. The identification of the spectrum of Pb^{3+} is based on

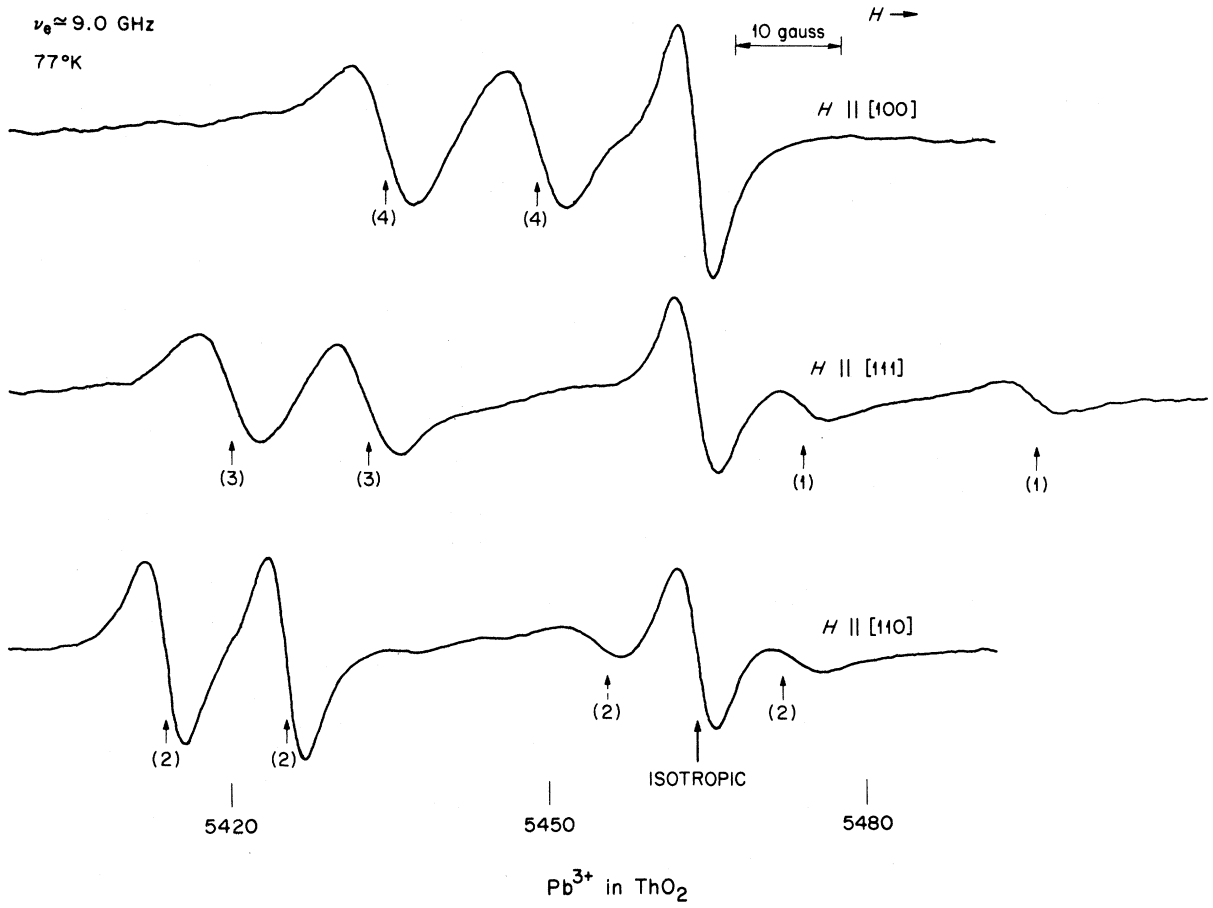

FIG. 2. ESR spectrum of electron irradiated ThO_2 showing the high-field hyperfine lines due to $^{207}Pb^{3+}$. The cubic line at 5470 G is isotropic, while the other lines which are due to the four ⟨111⟩ axially symmetric sites are split by a ^{19}F superhyperfine interaction. Linewidth variation with angle accounts for the apparent peak-to-peak intensity discrepancies.

TABLE I. Spin Hamiltonian parameters for the centers observed in irradiated ThO_2 and CeO_2.

Crystal	Type of irradiation	Center principal axes	g	A (cm^{-1})	A_F (10^{-4} cm^{-1})
ThO_2	β^- at 300 K	Pb^{3+} isotropic	$g = 1.9666 \pm 0.0006$	1.230 ± 0.005	···
ThO_2	β^- at 300 K	Pb^{3+}-F^- ⟨111⟩	$g_\parallel = 1.9704 \pm 0.0007$	$A_\parallel = 1.194 \pm 0.010$	$(A_F)_\parallel = 18.9 \pm 0.5$
			$g_\perp = 1.9637 \pm 0.0007$	$A_\perp = 1.181 \pm 0.010$	$(A_F)_\perp = 10.5 \pm 0.5$
CeO_2	β^- at 300 K	Pb^{3+} isotropic	$g = 1.9649 \pm 0.0008$	1.204 ± 0.005	···
ThO_2	Neutrons at 320 K	? ⟨100⟩	$g_\parallel = 1.812 \pm 0.001$	···	···
			$g_\perp = 1.925 \pm 0.001$		
ThO_2	Neutrons at 130 K	? ⟨111⟩	$g_\parallel = 2.003 \pm 0.001$	···	···
			$g_\perp = 2.095 \pm 0.001$		

several observations. The intensity of the spectra increased as the amount of Pb in the crystals increased; the zero-field splitting constant, or hyperfine interaction constant A is comparable to that observed for Pb^{3+} in KCl, [5] for Tl^{2+} (which is isoelectronic with Pb^{3+}) in KCl [6] and ZnS, [7] and for Pb^{3+} in $CaCO_3$. [8] The ratio of the intensity for both Pb^{3+} spectra of the lines near $g = 2$ to the intensity of the hyperfine lines near 5470 G agrees with the ratio of the isotopic abundances of the even-even Pb isotopes to ^{207}Pb. The effect of the neutron irradiation was to enrich the sample in ^{208}Pb, further confirming the identification of the high-field lines as Pb^{3+} hyperfine lines. The second hyperfine line, denoted H_2 in the Appendix, was not observed at 9 GHz, possibly because it was broadened in addition to being less intense; it cannot be seen when the microwave energy exceeds $\frac{1}{2}A$ (e.g., 34 GHz). Also, since for our 34-GHz spectrometer the microwave energy was less than A, we were unable to observe the transition from the singlet ground state to the upper triplet state.

It is believed that the lead goes into the crystals as Pb^{2+} (in a thorium site), some of which is converted to Pb^{3+} after irradiation, since divalent lead is more stable than tetravalent lead at the elevated temperatures required in the crystal growth procedure. After irradiation, the charge compensation for the cubic Pb^{3+} spectrum is evidently remote, while the presence of the $\langle 111 \rangle$ axially symmetric Pb^{3+} spectrum is consistent with the charge compensation (^{19}F) occurring in the first-neighbor oxygen site.

The ESR spectrum which Neeley *et al.*[2] measured at 25 GHz in ThO_2 crystals grown from PbF_2-based solvents had $\langle 111 \rangle$ axial symmetry with linewidths ranging from 32 G at room temperature to less than 1.5 G near liquid-helium temperatures. If we designate the superhyperfine lines of the $\langle 111 \rangle$ axial Pb^{3+} spectrum as A and B (Fig. 1), the "g values" of the A lines agree, within experimental error, with those which they reported for the "F center." Since in all of our experiments we have been unable to produce the set of lines designated A, or others similar to them, without the presence of the lines labeled B (or the isotropic Pb^{3+} line), it would appear that the previous identification of the spectrum of the F center in ThO_2 is questionable. Furthermore, in the alkali halides, alkaline-earth fluorides and oxides, the electron trapped at the negative-ion vacancy has a nonlocalized wave function. This results in ESR spectra with *isotropic* g values and linewidths which do not vary greatly with temperature. Moreover, in the alkaline-earth oxide compounds, ionizing radiation alone is not sufficient to produce F centers. Neutron or prolonged electron irradiations are required to form oxygen-ion vacancies by means of collision-displacement processes. [9] It would be difficult from an ESR spectrum alone to identify an F center in ThO_2 (if it were present), since there are no nuclei with spin to produce the hyperfine structure needed for a positive identification similar to the original work of Kip *et al.* [10]

The $\langle 100 \rangle$ axial symmetry of the new center observed in the 320-K neutron irradiated crystals shows that the interstitial site in the ThO_2 lattice must be involved. The occurrence of this center in all crystals, regardless of their impurity content, after neutron irradiation suggests that it is a lattice defect where, as a result of knock-on collisions, one of the lattice ions has been displaced to the interstitial site with the appropriate charge compensation occurring at an immediately adjacent thorium site. The complete lack of hyperfine structure in this center, however, makes it difficult to propose a model for it.

ACKNOWLEDGMENTS

The authors wish to express their appreciation to S. A. Marshall, who supplied crystals grown by Norton Industries, and J. M. Baker for the crystals grown by Barbara Wanklyn. The assistance of O. E. Schow with the electron irradiations is gratefully acknowledged. The authors are also indebted to R. A. Weeks and T. L. Purcell for their measurements on the low-temperature neutron irradiated sample.

APPENDIX

The Breit-Rabi[11] notation is that

$$\mathcal{H} = -g_I\beta\vec{H}\cdot\vec{I} - g_J\beta\vec{H}\cdot\vec{J} + A\vec{I}\cdot\vec{J} \quad .$$

For the case $J = \frac{1}{2}$, we have

$$E_{m_F} = -\frac{h\Delta\nu}{2(2I+1)} - g_I\beta H m_F \pm \tfrac{1}{2}h\Delta\nu\left(1 + \frac{4m_F X}{2I+1} + X^2\right)^{1/2} ,$$

where

$$h\Delta\nu = A(I+\tfrac{1}{2}), \quad X = -\left[(g_J - g_I)\beta H/h\Delta\nu\right] \quad .$$

We will neglect the nuclear Zeeman term and use the Hamiltonian

$$\mathcal{H} = g\beta\vec{H}\cdot\vec{S} + A\vec{I}\cdot\vec{S} \ .$$

For $S = \frac{1}{2}$ and $I = \frac{1}{2}$, the energies are found in Table II.

The observed high-field transition is the

$$|F = 1,\ m_F = 0\rangle \rightarrow |F = 1,\ m_F = -1\rangle \text{ transition.}$$

The energy separation is equal to the following:

$$h\nu = E_2 - E_3 = \tfrac{1}{2}g\beta H_1 - \tfrac{1}{2}A + \tfrac{1}{2}\left[(g\beta H_1)^2 + A^2\right]^{1/2} ,$$

$$(2h\nu - g\beta H_1 + A)^2 = (g\beta H_1)^2 + A^2 \ ,$$

TABLE II. Energy levels and quantum numbers for $S=\frac{1}{2}$ and $I=\frac{1}{2}$.

	Low-field quantum numbers		High-field quantum numbers	
	F	m_F	M_S	m_I
$E_1=\frac{1}{2}g\beta H+\frac{1}{4}A$	1	+1	$+\frac{1}{2}$	$+\frac{1}{2}$
$E_2=-\frac{1}{4}A+\frac{1}{2}\times[(g\beta H)^2+A^2]^{1/2}$	1	0	$+\frac{1}{2}$	$-\frac{1}{2}$
$E_3=-\frac{1}{2}g\beta H+\frac{1}{4}A$	1	−1	$-\frac{1}{2}$	$-\frac{1}{2}$
$E_4=-\frac{1}{4}A-\frac{1}{2}\times[(g\beta H)^2+A^2]^{1/2}$	0	0	$-\frac{1}{2}$	$+\frac{1}{2}$

$$A=\frac{(2h\nu)(h\nu-g\beta H_1)}{(g\beta H_1-2h\nu)} \quad \text{or} \quad g\beta H_1=\frac{2h\nu(h\nu+A)}{(2h\nu+A)} \tag{A1}$$

Another high-field transition should be observed for the

$$|F=1,\ m_F=1\rangle \rightarrow |F=1,\ m_F=0\rangle \text{ transition:}$$

$$h\nu=E_1-E_2=\tfrac{1}{2}g\beta H_2+\tfrac{1}{2}A-\tfrac{1}{2}\{[(g\beta H_2)^2+A^2]\}^{1/2},$$

$$(2h\nu-g\beta H_2-A)^2=(g\beta H_2)^2+A^2, \tag{A2}$$

$$g\beta H_2=2h\nu(h\nu-A)/(2h\nu-A).$$

Taking formulas (A1) and (A2) and setting

$$g=\frac{2h^2\nu^2-2h\nu A}{(2h\nu-A)\beta H_2}=\frac{2h^2\nu^2+2h\nu A}{(2h\nu+A)\beta H_1},$$

we may cross multiply and solve for A,

$$A=[h\nu/2(H_2-H_1)]\{(H_2+H_1)\pm[(H_2+H_1)^2+8(H_2-H_1)^2]^{1/2}\}. \tag{A3}$$

The transition probabilities for the two lines show that the line at H_2 for $\nu\simeq 9$ GHz, which should appear at ~10450 G, is lower in intensity by a factor of ~3.5 from the line at H_1 (~5700 G). If the hyperfine interaction has axial symmetry, then the final expressions for $A_\parallel$ and $A_\perp$, in terms of H_1, are

$$A_\parallel=\frac{(2h\nu)[h\nu-g_\parallel\beta H_1]+\frac{1}{2}(A_\parallel^2-A_\perp^2)}{[g_\parallel\beta H_1-2h\nu]},$$

$$A_\perp=\frac{(2h\nu)[h\nu-g_\perp\beta H_1]+\{\frac{1}{2}A_\perp^2-\frac{1}{2}[\frac{1}{2}(A_\parallel+A_\perp)]^2\}}{[g_\perp\beta H_1-2h\nu]}. \tag{A4}$$

†Research sponsored by the U. S. Atomic Energy Commission under contract with Union Carbide Corporation.

[1]W. Low and D. Shaltiel, Phys. Rev. 115, 424 (1959).
[2]V. I. Neeley, J. B. Gruber, and W. J. Gray, Phys. Rev. 158, 809 (1967).
[3]A. B. Chase and J. A. Osmer, Am. Mineralogist 49, 1469 (1964).
[4]C. B. Finch and G. W. Clark, J. Appl. Phys. 36, 2143 (1965).
[5]D. Schoemaker and J. L. Kolopus, Solid State Commun. 8, 435 (1970).
[6]W. Dreybrodt and D. Silber, Phys. Status Solidi 20, 337 (1967).
[7]A. Räuber and J. Schneider, Phys. Status Solidi 18, 125 (1966).
[8]R. M. Mineeva and L. V. Bershov Fiz. Tverd. Tela 11, 803 (1969) [Soviet Phys. Solid State 11, 653 (1969)].
[9]B. Henderson and J. E. Wertz, Advan. Phys. 17, 749 (1968).
[10]A. F. Kip, C. Kittel, R. A. Levy, and A. M. Portis, Phys. Rev. 91, 1066 (1953).
[11]G. Breit and I. I. Rabi, Phys. Rev. 38, 2082 (1931); N. F. Ramsey, *Molecular Beams* (Clarendon Press, Oxford, 1956).

PHYSICAL REVIEW B VOLUME 2, NUMBER 6 15 SEPTEMBER 1970

Empirical Relation between the Linear and the Third-Order Nonlinear Optical Susceptibilities

Charles C. Wang
Scientific Research Staff, Ford Motor Company, Dearborn, Michigan 48121
(Received 3 February 1970)

A simple empirical relation is found to exist between the linear and the third-order nonlinear optical susceptibilities. This empirical relation holds within the available experimental accuracy for gases at low pressures. The applicability of this empirical relation to crystalline solids, and its bearing on the generalized Miller's rule for these solids, are discussed.

In this article we wish to report on an empirical relation between the linear and the third-order nonlinear optical susceptibilities of gases at low pressures. This empirical relation makes use of the